Materials Transactions, Vol. 48, No. 12 (2007) pp. 3062 to 3065
Special Issue on Growth of Ecomaterials as a Key to Eco-Society III

Unburned Carbon Behavior in Sintered Coal Fly-Ash Bulk Material by Spark Plasma Sintering

Kazuhiro Hasezaki[1], Akifumi Nakashita[2], Gen-yo Kaneko[1] and Hideaki Kakuda[2]

[1]*Department of Materials Science, Shimane University, Matsue 690-8504, Japan*
[2]*The Chugoku Electric Power Co., Inc., Hiroshima 730-870, Japan*

Coal fly-ash bulk materials were prepared by spark plasma sintering (SPS). The as-received coal fly ash produced by Misumi Power Station (The Chugoku Electric Power Co., Inc.), had an average particle size of 19 μm and contained about 2% carbon from unburned coal. The sintering temperature was 1000°C for 10 min. The mass density of the sintered compact was 2.4×10^3 kg/m^3. After three-point flexural testing of the compact, the average flexural strength and Young's modulus were 25.6 MPa and 23.0 GPa, respectively. From the flexural strength, the Weibull modulus was found to be $m = 6.13$, indicating that the compact was a typical ceramics. Fractographic examination indicated that in all specimens the fracture origin was located on the bottom surface and was not an intrinsic flaw. Vickers indentation test showed that the fracture toughness was 0.61 MPa·m$^{0.5}$ and the calculated critical flaw size, c_0, was 0.18 mm. This c_0 value was larger than that of the voids and unburned carbon on the fracture surface. It is noteworthy that the mechanical strength of the sintered compact was not affected by the voids and unburned carbon. [doi:10.2320/matertrans.MK200702]

(Received April 11, 2007; Accepted June 1, 2007; Published November 25, 2007)

Keywords: *coal fly ash, spark plasma sintering, flexural strength, critical flaw size, Vickers indentation, recycling*

1. Introduction

The management of coal fly ash produced by coal thermal power stations is a major problem in many parts of the world. However, its generation tends to increase every year. Although some coal fly ash is used in a range of applications, particularly as a substitute for cement in concrete, large amounts remain unused and thus require disposal. At present, coal fly ash is used in civil engineering for the production of cement, concrete, porous brick and artificial aggregate,[1–5] and is also used in fertilizer systems.[6–8] These methods use coal fly ash simply as a powder, but it is hoped that more advanced and effective uses can be found in various fields to realize its full value.

When coal fly ash is sintered in a furnace under air,[9] carbon dioxide is produced from the residual unburned carbon, and the sintered compact deteriorates due to the presence of many gasified pores. Spark plasma sintering (SPS) is a well known technique for the preparation of sintered compact under a vacuum, providing high-density sintering and a short sintering time. It also has the potential to prevent the formation of many gasified pores.

This study investigated the sintering and mechanical properties of coal fly ash prepared by SPS.

2. Experimental

Coal fly ash was the source powder used to prepare the sintered materials. The coal fly ash, which was produced by Misumi Power Station (The Chugoku Electric Power Co., Inc.), had an average particle size of 19 μm. Its chemical composition is shown in Table 1. It also contained about 2% unburned carbon from pulverized coal.

Thermal analysis of the coal fly ash was performed using a RIGAKU Thermo Plus thermogravimetrical-differential thermal analyzer (TG-DTA) under air or nitrogen flow at 100 sccm, with a heating rate of 20 K/min and alumina as the standard.

Table 1 Chemical compositions of coal fly ash from Misumi Power Station.

Composition	Mass %
SiO_2	63.5 ± 5.1
Al_2O_3	22.5 ± 3.0
Fe_2O_3	4.3 ± 1.0
CaO	1.8 ± 1.3
MgO	0.8 ± 0.4
SO_3	0.3 ± 0.1
Na_2O	0.6 ± 0.3
K_2O	1.0 ± 0.3
C	2.0–4.0

Sintering was performed using the SPS apparatus (SS-Alloy Co. Ltd). The coal fly ash was put in a graphite die of 10 or 100 mm diameter and a mechanical pressure of 50 MPa was applied to the graphite punches. Sintering was performed at 800–1100°C for 10 min with a pulse current. The sintered materials were then cooled to room temperature over 30 min. This process was performed under a vacuum (10 Pa). The temperature was measured by a radiation pyrometer. The sintering conditions were monitored from the displacement of the upper electrode.

The density of the sintered materials was measured by the Archimedes method. Phase identification of the coal fly ash compact sintered at 1000°C was performed by X-ray diffraction (RINT2500HD/PC) using Cu-K_α radiation. Scanning electron microscopy (SEM) and electron probe micro-analysis (EPMA) were undertaken using a JEOL JXA-8800M.

The maximum size of the compact was 5 mm thickness × 100 mm diameter. After machining the compact into specimens (42 mm × 4.0 mm × 3.0 mm), 14 specimens underwent three-point flexural testing with a cross-head speed of 0.5 mm/min[10] using a SHIMAZU AG-100kNG according to the procedure of JIS R 1601. The fractured surfaces of all

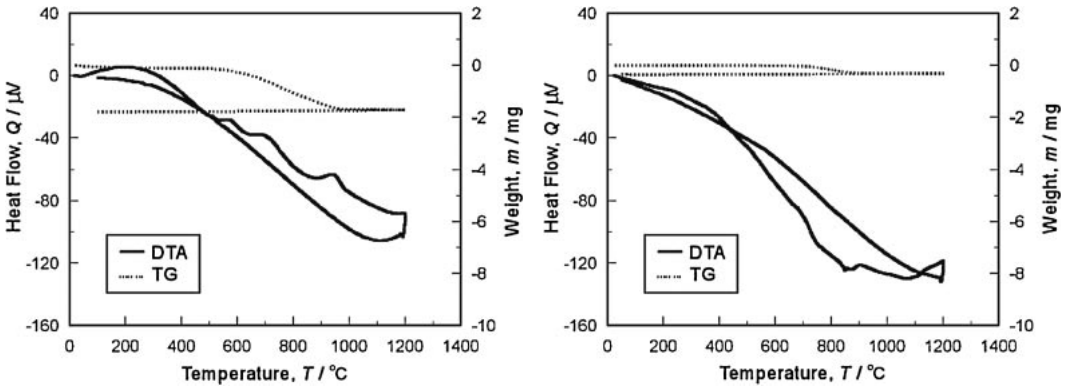

Fig. 1 TG-DTA curves of raw powders in (a) air and (b) nitrogen flow.

specimens were examined with an optical microscope to identify the fracture origin and flaws. Young's modulus was estimated from the load-displacement curve. The flexural strength, σ, was evaluated using the Weibull distribution function in eq. (1),

$$P_f = 1 - \exp\left\{-\left(\frac{\sigma}{\sigma_0}\right)^m\right\}, \quad (1)$$

where P_f is the probability of fracture and σ_0 is the characteristic strength value.[11] The Weibull modulus m is a measure for the scatter of strength data; the wider the distribution becomes, the smaller the value of m.

The Vickers hardness and fracture toughness were examined using an AKASHI AAV502 according to the procedure of JIS R 1607, with a load and loading time of 300 gf and 10 s, respectively. The fracture toughness, K_{1c}, is given by eq. (2),

$$K_{1c} = 0.026\left(\frac{E \cdot P}{C^3}\right)^{1/2} a, \quad (2)$$

where E is the Young's modulus (Pa), P is the indentation load (gf), C is the radial half crack length (m) and a is the indentation half crack length (m).[12]

3. Results and Discussion

Figure 1 shows the TG-DTA curves of the as-received coal fly ash in (a) air and (b) nitrogen flow. The DTA curve (a) in air flow shows three exothermic peaks at 580, 700 and 950°C during the heating process, while no exothermic peak was observed during the cooling process. Thus, the exothermic peaks were attributable to an irreversible reaction. The TG curve in air began to decrease at 580°C and reached a steady state at over 950°C. In nitrogen flow (b), two exothermic peaks in the DTA curve were observed at 700 and 950°C. The TG curve began to decrease at 700°C and reached a steady state at over 950°C. It is speculated that the exothermic peak at 580°C in air was due to combustion of the unburned carbon in the coal fly ash, which led to a mass decrease. The exothermic peaks at 700 and 950°C could have resulted from evaporation of Na_2O and K_2O alkali oxides of low melting point and crystallization of the glass phase. From these thermal properties, the optimal sintering conditions were judged to be in a vacuum at over 1000°C.

In addition, the mass density was measured for coal fly ash compact sintered by SPS in the temperature range 800–1100°C. Figure 2 shows a plot of the mass density of the sintered compact against the sintering temperature. The mass density was saturated at 2.4×10^3 kg/m^3 over 1000°C. The results shown in Figure 1 and 2 support the optimal SPS sintering conditions of 1000°C in a vacuum. Figure 3 shows SEM micrographs and the EPMA elemental distribution of the cross-section of coal fly ash compact sintered by SPS at 1000°C. Cracks and pores were difficult to detect by SEM (a). From the elemental distribution (b–d) and X-ray diffraction pattern, the sintered compact was determined to be made up of multiple phases, which were identified to be mullite ($3Al_2O_3 \cdot 2SiO_2$) and silica (SiO_2), corresponding to the composition shown in Table 1. In the central portion (60 μm) of the low signal area, the detected constituents were possibly unburned carbon from pulverized coal.

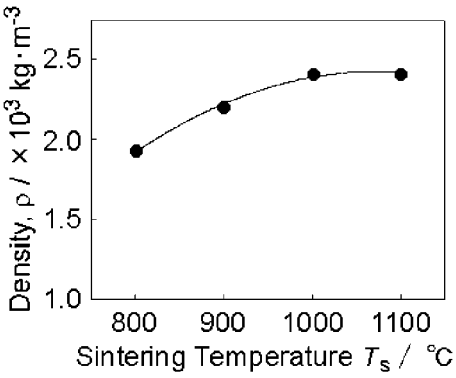

Fig. 2 Mass density of coal fly ash prepared by SPS plotted in terms of sintering temperature.

After three-point flexural testing, the fractured surfaces of the 14 test specimens were examined by optical microscopy to identify the fracture origin. Figure 4 shows a typical fractographic examination of sintered compact after the three-point flexural test; (a) shows the fracture origin and (b) a void and unburned carbon on the fracture surface. The fracture origin was located on the bottom surface and could not be attributed to the defects shown in (b). The average sizes of the unburned carbon and voids on the fracture surface were 60 μm and 80 μm, respectively. The size of the unburned carbon was equivalent to that of the low signal area in Fig. 3(a)–(d).

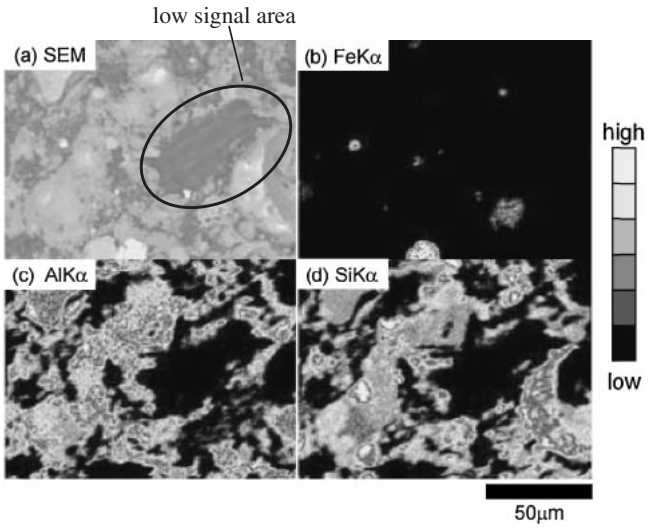

Fig. 3 (a) SEM micrograph and (b–d) EPMA elemental distribution of sintered compact.

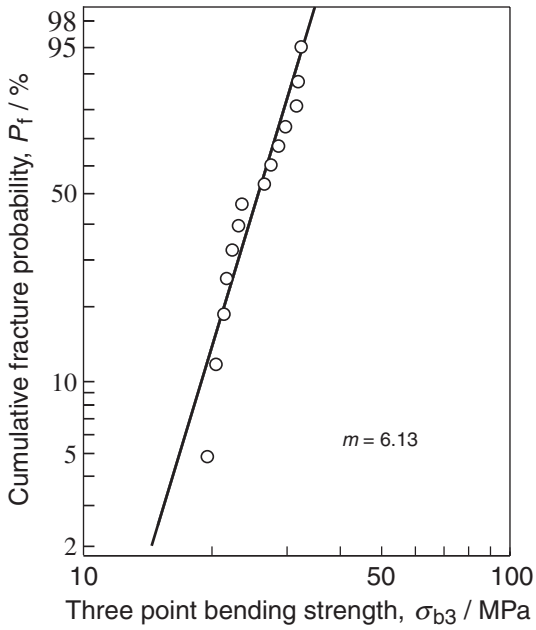

Fig. 5 Weibull flexural strength distribution plots for sintered compacts.

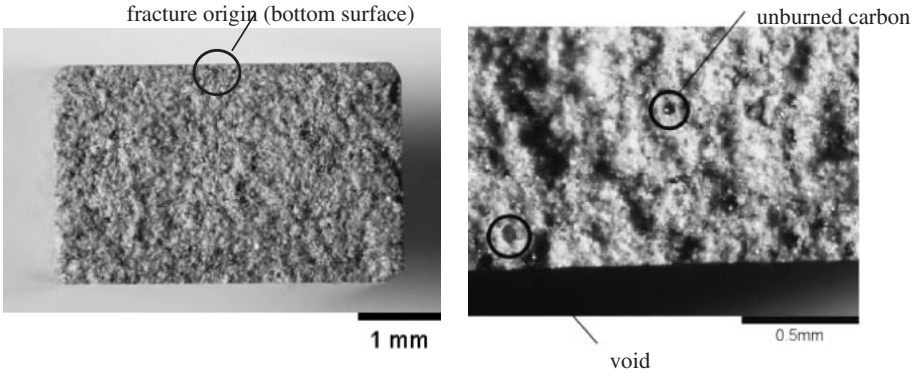

Fig. 4 The fractographic examination of sintered compact after the three point bending test. (a) fracture surface, (b) void and unburned carbon.

Figure 5 shows a Weibull plot for all of the flexural strength data. The average flexural strength and Young's modulus were estimated to be 25.6 MPa and 23.0 GPa, respectively. From the linear relationship between mechanical load and the probability of failure, the Weibull modulus was calculated to be $m = 6.13$ by the least squares method; this value corresponds to that of a typical ceramics.

Figure 6 shows the Vickers indention test; (a) shows the characteristic length of cracks and (b) is an optical microphotograph of the sintered compact. The observed mechanical properties are summarized in Table 2. The Vickers hardness was 630–681 Hv and the fracture toughness was evaluated to be 0.61 MPa·m$^{0.5}$. The critical flaw size, c_0, is given by eq. (3),

$$c_0 = \frac{K_{1c}^2}{\pi\sigma^2}, \tag{3}$$

where K_{1c} and σ are the fracture toughness and average three-point bending stress, respectively. From these properties, the critical flaw size, c_0, can be estimated to be 0.18 mm. The observed c_0 is larger than that of the void and unburned carbon on the fracture surface in Fig. 4(b). From these findings, it is notable that the unburned carbon in the sintered compact undoubtedly did not affect its mechanical strength.

4. Conclusions

This study investigated the sintering and mechanical properties of coal fly ash compact prepared by SPS. The results were as follows.

(1) The coal fly ash could be sintered using SPS at 1000°C for 10 min with a resultant mass density of 2.4×10^3 kg/m^3.
(2) The average flexural strength and Young's modulus were 25.6 MPa and 23.0 GPa, respectively. The Weibull modulus was $m = 6.13$, indicating that the material was a typical ceramics.
(3) On fractographic examination of the sintered compact after three-point flexural testing, the fracture origin was found on the bottom surface, and was not an intrinsic flaw, in all of the tested specimens.

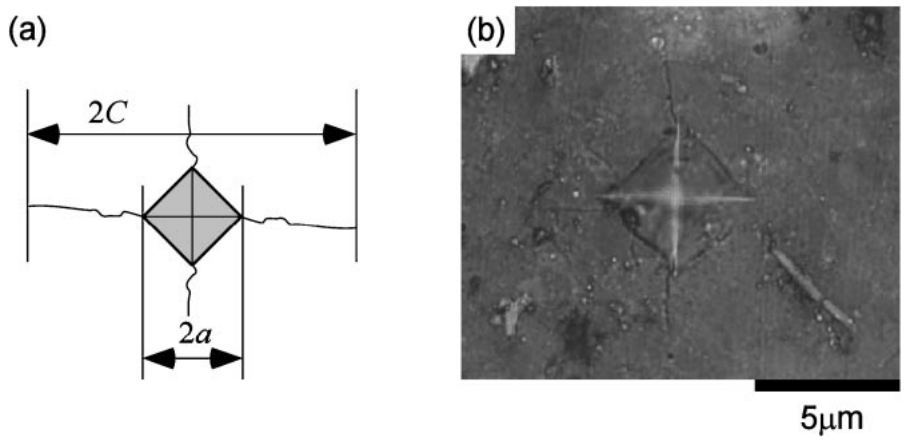

Fig. 6 Vickers indentation test of (a) characteristic lengths of the cracks and (b) optical microphotograph of sintered compact of coal fly ash.

Table 2 Summary of mechanical properties for sintered compacts of coal fly ash prepared by SPS at 1000°C.

Material	Density ρ (kg/m^3)	Average three point bending stress σ_b (MPa)	Average Young's modulus, E (GPa)
Sintered compact of coal fly ash	2.4×10^3	25.6	23.0
	Weibull modulus m	Vickers hardness (Hv)	Fracture toughness K_{Ic} (MPa·m$^{0.5}$)
	6.13	630–681	0.61

(4) Using the observed fracture toughness, K_{1c}, of 0.61 MPa·m$^{0.5}$, the critical flaw size, c_0, was estimated to be 0.18 mm, which is larger than the voids and unburned carbon on the fracture surface. It is noteworthy that the mechanical strength of the sintered compacts was not affected by the small voids and unburned carbon.

Acknowledgement

We thank Sakae Mishima, Yoshiaki Suzuki and Kazuki Kikui of Industrial Research Institute of Tottori Prefecture for mechanical testing.

REFERENCES

1) S. H. Lee, H. J. Kim, E. Sakai and M. Daimon: Cement and Concrete Research **33** (2003) 763–768.
2) A. Oner, S. Akyuz and R. Yildiz: Cement and Concrete Research **35** (2005) 1165–1171.
3) C. Berryman, J. Zhu, W. Jensen and M. Tadros: Cement and Concrete Research **35** (2005) 1088–1091.
4) M. J. McCarthy and R. K. Dhir: Fuel **84** (2005) 1423–1432.
5) R. S. Iyer and J. A. Scott: Conservation and Recycling **31** (2001) 217–228.
6) M. R. Khan and M. W. Khan: Environmental Pollution **92** (1996) 105–111.
7) S. K. Rautaray, B. C. Ghosh and B. N. Mittra: Bioresource Technology **90** (2003) 275–283.
8) L. P. Singh and Z. A. Siddiqui: Bioresource Technology **86** (2003) 73–78.
9) M. Ilic, C. Cheeseman, C. Sollars and J. Knight: Fuel **82** (2003) 331–336.
10) Testing method for flexural strength (modulus of rupture) of fine ceramics. JIS R 1601, 1995.
11) W. Weibull: *A statistical theory of strength of materials*, (Royal Swedish Institute for engineering Research, 1939) pp. 1–45.
12) Testing method for fracture toughness of high performance ceramics. JIS R 1607, 1990.